ELSEVIER

Journal of Power Sources 113 (2003) 200–208

JOURNAL OF POWER SOURCES

www.elsevier.com/locate/jpowsour

Progress in overcoming the failure modes peculiar to VRLA batteries

A. Cooper[a], P.T. Moseley[b,*]

[a]EALABC (EEIG), 42 Weymouth Street, London W1G 6NP, UK

[b]International Lead Zinc Research Organization, P.O. Box 12036, Research Triangle Park, NC 27709, USA

Abstract

The results of an international collaborative program of research have shed new light on the mechanisms limiting the life of valve-regulated lead–acid (VRLA) batteries under different duty cycles. Management of the internal oxygen cycle is a central issue and improvements in materials selection and cell design show promise of significant extension in battery life.

Keywords: Lead–acid batteries; VRLA; Separators; Negatives plate; Tubular plates

1. Introduction

The valve-regulated lead–acid (VRLA) battery differs from its flooded electrolyte precursor in a number of important ways [1]. In the VRLA battery, the electrolyte is immobilized so that the possibility of acid leakage is greatly reduced. The tendency for hydrogen gas to be generated at the negative plate is reduced by the elimination of antimony from the alloys employed in the grid construction. Finally, the cell is closed, apart from a pressure release valve, and an internal oxygen cycle provides that very little gas (hydrogen, oxygen or both) is lost to the outside atmosphere even during overcharge. Since its introduction in the 1960s, the VRLA battery has been progressively displacing the flooded battery from many applications because it offers a number of advantages [2]. These include reduced maintenance operation in any orientation and higher specific energy at high discharge rates. The reactions, which are called up during the operation of a VRLA cell are shown in Table 1.

Reactions (1)–(4) are the intended discharge and recharge reactions of the positive and negative plate respectively. Reactions (5) and (8) are the gassing reactions which occur towards the top of charge on the positive and negative plate freely and which lead to the loss of water from the electrolyte of flooded batteries. Reaction (6) represents the corrosion of the positive plate, which also consumes water. In VRLA cells, the reduction of oxygen at the negative plate (reaction (7)) must also be taken into account. These four 'secondary' reactions (5)–(8) constitute inefficiency in the charging process and are involved in processes which degrade the performance of the cell.

During the period January 1998 to August 2001, the European component of the Advanced Lead–Acid Battery Consortium (ALABC) carried out a coordinated international program of research to address the factors which were limiting the performance of VRLA batteries at each stage of their life [3]. The purpose of the project has been to provide remedies so that the battery would be able to perform all the duties required of it for an economically valuable service life. The prime objective was to extend the life of the battery in the deep cycle application required for electric vehicle duty, but much of the development which has been achieved will also be of value to the use of the battery in other applications.

2. VRLA failure modes

The mechanisms which limit the life of the VRLA battery (failure modes) are somewhat different from those which limit the performance of the flooded battery. The failure modes also vary with the application since different duties involve quite different depths of discharge and rates of charge and discharge (Table 2).

2.1. Premature capacity loss (PCL)-1

Early attempts to operate VRLA batteries in deep discharge duty resulted in failure after only a relatively small number of discharge/recharge cycles. The cause of this early failure, which was termed "premature capacity loss" (PCL)

* Corresponding author. Tel.: +1-919-361-4647; fax: +1-919-361-1957.
E-mail address: 72254.521@compuserve.com (P.T. Moseley).

0378-7753/02/$ – see front matter © 2002 Published by Elsevier Science B.V.
PII: S0378-7753(02)00515-3

Table 1
Reactions taking place during discharge and recharge of a VRLA cell

Reactions occurring during discharge		Reactions occurring during charge	
$PbO_2 + 3H^+ + HSO_4^- + 2e^- \rightarrow PbSO_4 + 2H_2O$	(1)	$PbSO_4 + 2H_2O \rightarrow PbO_2 + 3H^+ + HSO_4^- + 2e^-$	(3)
$Pb + HSO_4^- \rightarrow PbSO_4 + H^+ + 2e^-$	(2)	$PbSO_4 + H^+ + 2e^- \rightarrow Pb + HSO_4^-$	(4)
		$2H_2O \rightarrow 4H^+ + O_2 + 4e^-$	(5)
		$Pb + 2H_2O \rightarrow PbO_2 + 4H^+ + 4e^-$	(6)
		$O_2 + 4H^+ + 4e^- \rightarrow 2H_2O + \text{heat}$	(7)
		$2H^+ + 2e^- \rightarrow H_2$	(8)

Table 2
Typical rates of discharge and charge and ranges of state-of-charge for the range of duty cycles

Duty	Float	Deep discharge	Low rate PSoC	High rate PsoC	SLI
Examples	UPS	EV	RAPS	HEV/36 V	12 V
Range of SoC	N/A	20–100	40–90	50–60	95–100
Maximum normal rate discharge[a]	5	0.5	0.2	15	5
Maximum normal rate of charge[a]	0.05	0.5	0.2	8	0.05

[a] In multiples of the 1 h rate.

stemmed from a high resistance arising in the vicinity of the interface between the active material and the surface of the grid of the positive plate [1]. This failure mode appeared to be linked with the changes which were made to grid alloy composition in the VRLA design and the problem has been largely overcome by the incorporation of tin in the antimony-free alloys. In the light of subsequent findings, it is becoming common practice to refer to this phenomenon as PCL-1.

2.2. Premature capacity loss (PCL)-2

Once the interface problem had been overcome, VRLA batteries in deep cycle duty were able to provide a service life of several hundred cycles, and it was found that a new failure mode was limiting their ability to approach the deep cycle lifetime offered by flooded cells. The new problem resided within the body of the positive active mass (PAM). During discharge, the PAM undergoes a large solid volume increase as a result of the conversion of PbO_2 to $PbSO_4$, and, although this volume change tends to be reversed during a single recharge, the overall effect of the deep cycling process is a progressive swelling and a loss of cohesion. As with flooded batteries, this failure mode can be ameliorated by the application of pressure on the plate stack [4]. This tactic is less successful with VRLA cells, however, since the separator designed to immobilize the electrolyte is compressible and able to absorb much of the stack compression which is intended to constrain the active mass. This failure mode, which is characterized by a softening of the positive active mass revealed in tear-down analysis, has been labeled ‘PCL-2’.

2.3. Premature capacity loss (PCL)-3

More recently, a further failure mechanism has appeared to limit the life of VRLA cells. In some batteries, in which the effects of PCL-2 have been overcome sufficiently for a life approaching 1000 deep cycles to be achieved, and in others which are serving high rate partial-state-of-charge (PSoC) duty, it appears that failure occurs due to sulphation of the negative plate. In the case of high rate PSoC, this failure can occur quite early in life. There is a growing body of opinion that this process arises when too much oxygen, evolved from the positive plate arrives at the negative plate where it is reduced, generating heat and dragging the potential more positive so that charging of the plate is hindered [5]. Following the developing convention it might be appropriate to term this mechanism ‘PCL-3’.

3. Program results

3.1. Positive grid

In the course of helping to overcome PCL-1, the addition of tin to antimony-free alloys substantially reduces the rate of corrosion of the grid. Thus, the allowance that has to be made in grid weight to accommodate a lifetime of corrosion can be reduced. It is thus possible to take advantage of these alloys by designing lighter grids and thereby achieving improvement in specific energy. During the course of the present program batteries with lightweight novel tubular plates have been produced and shown to give good performance [6]. Positive plates were constructed around grids with elliptical cross-section spines in order to provide an enhanced ratio of active mass weight/spine surface area (the so-called ‘gamma’ parameter). Spines with cross-sectional dimensions of 2.24 mm × 1.20 mm were used in cells which yielded 29 Wh/kg in the demanding ECE15L test. This represents a 60% improvement over existing tubular products and stands within the performance range of pasted

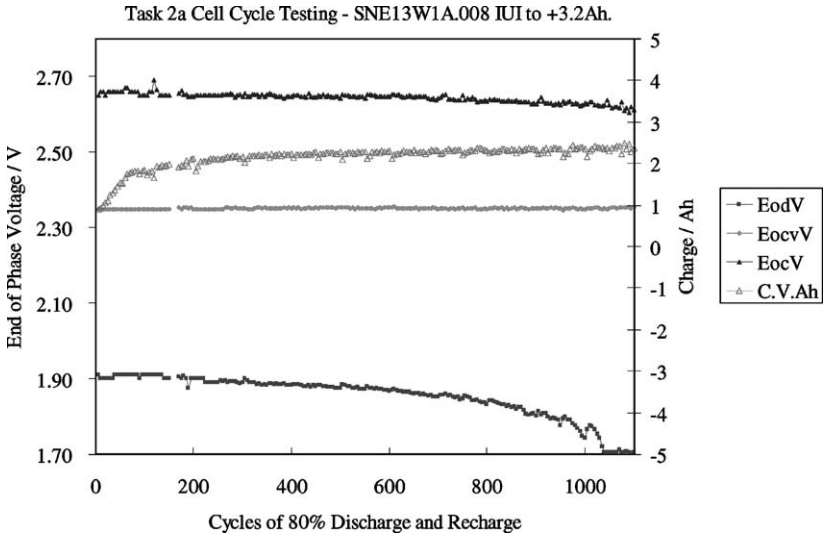

Fig. 1. Cycle life of cell with a tubular positive constructed with a spine of cross-sectional dimensions 2.24 mm × 1.20 mm [3].

plate valve-regulated batteries. The important element which tubular designs bring is a long service life. The cells with the present design showed 1000 cycles of 80% discharge and recharge (Fig. 1). The eventual failure mode was water loss.

Corrosion resistant grid alloys must be used with caution however since if there is too little interaction between the grid and the active mass then adhesion may be lost and capacity lost as a result [7]. When complete batteries were manufactured with the cell design mentioned above, a delay arose in the assembly process and this was sufficient to result in performance which was significantly less impressive than that of the cells. Diagnostic tests indicated that the positive plate performance was reduced in a manner which was reminiscent of thermopassivation. It seems that great care has to be taken to achieve the correct balance between low corrosion and adequate adhesion of the active material to the grid [7]. This latter factor is likely to be influenced both by the grid alloy chemistry and by process variables.

An additional benefit arising from the use of thin grid members and concomitant thin active material layers is that cells with tubular positive plates such as those described here are able to be fast charged [8], whereas cells with conventional tubular plates behave rather badly under a fast charge regime.

After a long cycling test with fast charging, cells with tubular positive plates became negative-limited and teardown analysis showed a greater accumulation of sulfate in the negative than in the positive plate, especially near the bottom of the plate [8].

3.2. Separator

The material used as the separator in VRLA cells exercises a crucial influence on the performance of both plates. A tendency to be easily crushed will allow the ready progress of PCL-2 while a microstructure which does not allow the electrolyte to provide an adequate barrier to oxygen transfer will allow the progress of PCL-3.

A laboratory experiment carried out at the University of Kassel [9] has helped to shed light on the nature and the function of the separator materials. A measurement of the force generated by the expansion of the active material during discharge and recharge has provided the results shown in Fig. 2a (negative plate) and Fig. 2b (positive plate). Fig. 2a shows that the forces arising in the negative plate are large, but reversible, while Fig. 2b shows that the forces arising in the positive active material are progressive. In both cases, however, the addition of a standard AGM separator material sees the forces largely absorbed.

Of course, it is the electrolyte within the pores of the separator that completes the barrier to the passage of oxygen from the positive to the negative plate. This is well illustrated in Fig. 3 which shows that, as separator becomes progressively more saturated with electrolyte so the cell potential rises to the gassing voltage at an earlier and earlier apparent state-of-charge [8].

During the course of the present program, four distinct approaches have been investigated in pursuit of a material to perform better than the incumbent grades of absorptive glass mat (AGM). The materials evaluated were as follows.

(A) A microporous membrane sandwiched between two layers of fine fibre AGM.
(B) A layered composite of two grades of AGM with the fine grade in contact with the electrodes and an inner part made of a coarse grade.
(C) A blend of AGM and organic fibers.
(D) A novel material with a very high silica content, labeled ‘acid jellifying separator’ or ‘AJS’.

Some considerable progress was made towards overcoming PCL-2 and, in these tests, no evidence was found that the

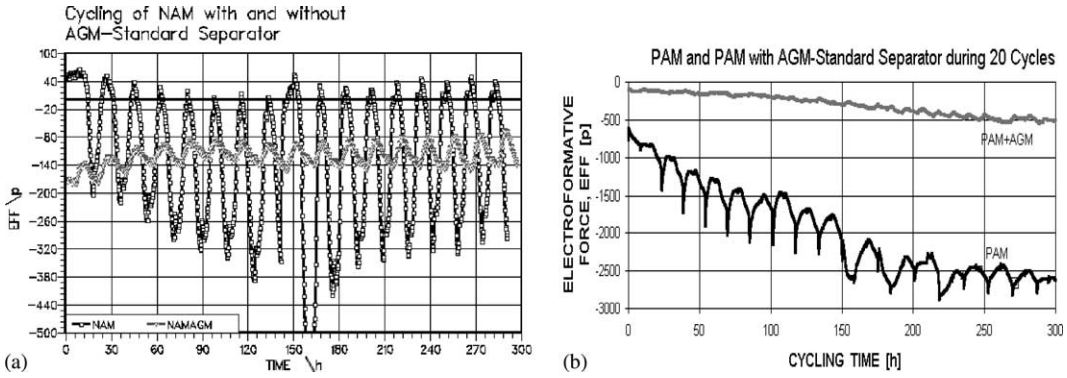

Fig. 2. Force fluctuation in the negative (a) and positive (b) plates, with and without separator present through a number of discharge/recharge cycles.

test objects had reached a stage where PCL-3 was the life limiting factor.

Fig. 4 shows the cycling performance of materials A and B subjected to continuous 100% depth-of-discharge cycling at the 5 h rate [10]. Material A performed the better of the two, achieving some 650 cycles to a cut-off at 80% of initial capacity. It should be pointed out, however, that the cell containing material B (which achieved rather less than 400 cycles) was only subjected to a compression of 30 kPa, while material A was compressed to 50 kPa.

Both cells drew overcharge factors which were constant during normal cycling at close to 10%. During capacity tests higher overcharge factors were used and over the last 150 cycles the cell with material A drew a steadily increasing overcharge which was matched by a high weight loss (Fig. 5).

Tear-down analysis showed no evidence for acid stratification or for short circuits. The cell with material A exhibited positive grid corrosion and some softening of the positive active mass. The cell with material B showed some positive active mass softening but in three distinct horizontal zones one above the other.

Fig. 6 shows the cycle life of a cell containing separator material C subjected to continuous 100% depth-of-discharge cycling at the 5 h rate [10]. The discharge capacity falls almost continuously to reach a value of 80% of initial after 700 cycles. The overcharge factor during cycling throughout was constant at close to 12% and, again, the failure mode was softening of the positive active mass particularly at the bottom of the plates. There was no evidence of stratification and no abnormal corrosion weight loss.

A further laboratory experiment at the University of Kassel [9] has served to point up the difference in wicking characteristics between materials A on the one hand and materials B and C on the other (Fig. 7). Material A is capable of maintaining saturation to a much greater height than the other two materials although its capacity per unit surface area is somewhat less. This property doubtless contributes to

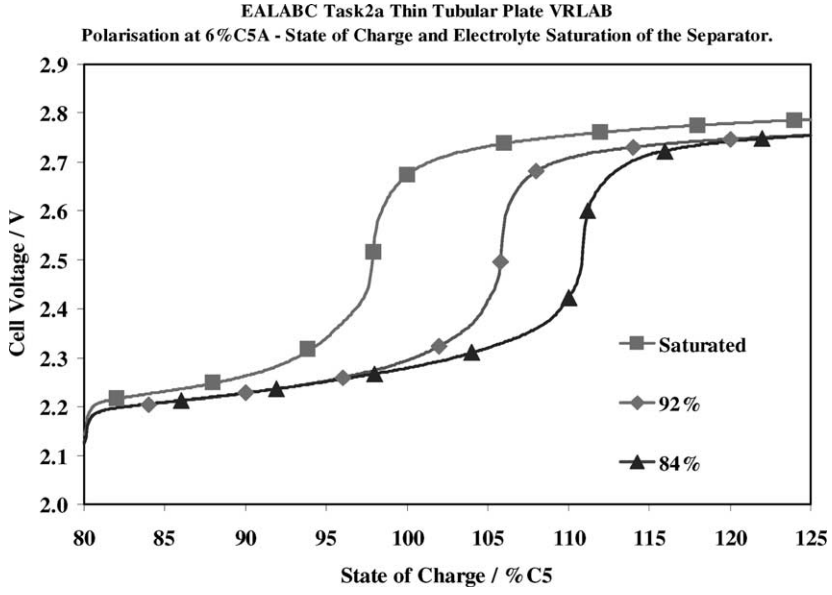

Fig. 3. Electrolyte saturation influence on oxygen cycle, recharge response and capacity.

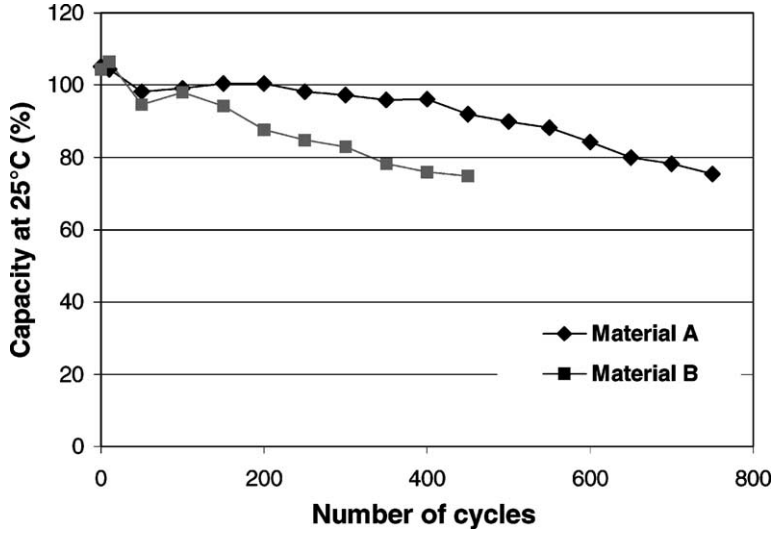

Fig. 4. Cycle life of cells containing separator materials A (compressed to 50 kPa) and B (compressed to 30 kPa).

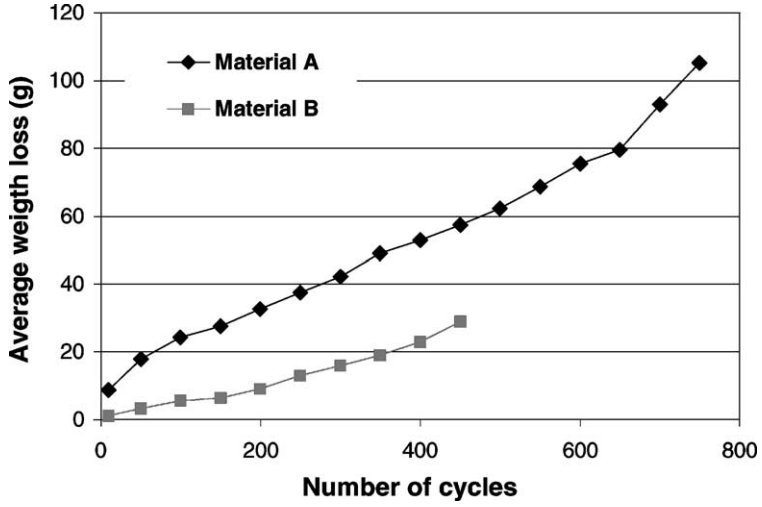

Fig. 5. Weight loss with time for cells containing separator materials A and B.

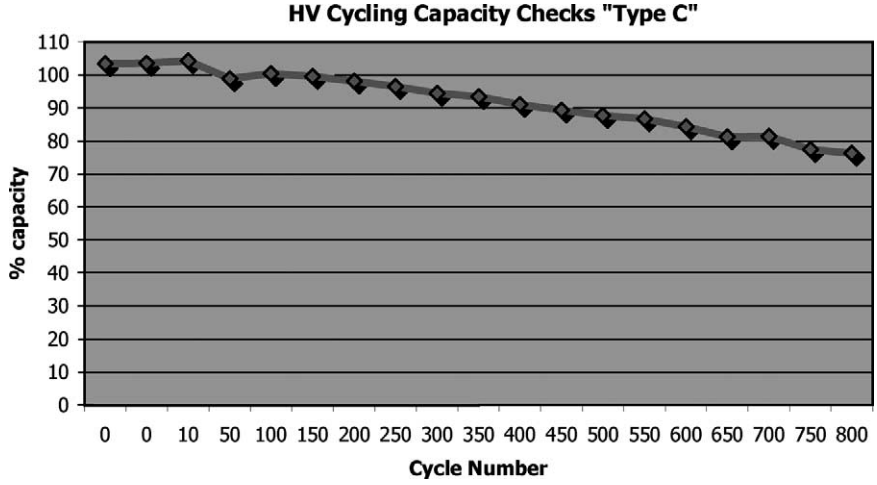

Fig. 6. Cycle life of cell containing separator material C (compressed to greater than 50 kPa).

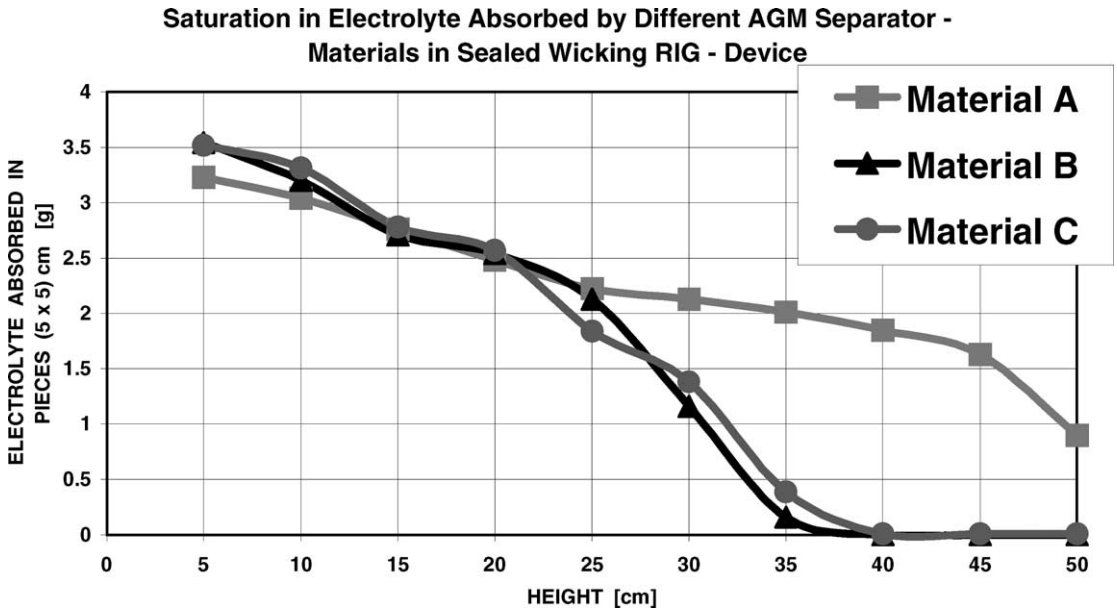

Fig. 7. Wicking characteristics of materials A, B, and C.

the ability of the material to restrict the transfer of oxygen across the cell and this accounts for the higher weight loss shown in Fig. 5.

The high-silica material, AJS, has a somewhat lower porosity (81%) than most grades of AGM, but the principal difference is that the pores are very much finer—mean size 0.2 μm as compared with a few microns in AGM. As a result, the graph of apparent diffusion coefficient of oxygen through the material as a function of saturation (Fig. 8), is quite different from that of AGM [11]. Fig. 9 shows the cycle life of a 50 Ah cell containing AJS as separator (compressed to 80 kPa) exposed to continuous 100% depth-of-discharge cycling at the 5 h rate. The charge factor remained around 10% for most of the test with this material. Tear-down analysis [11] provided evidence that the failure mode which terminated the test of these cells was corrosion of the positive grid

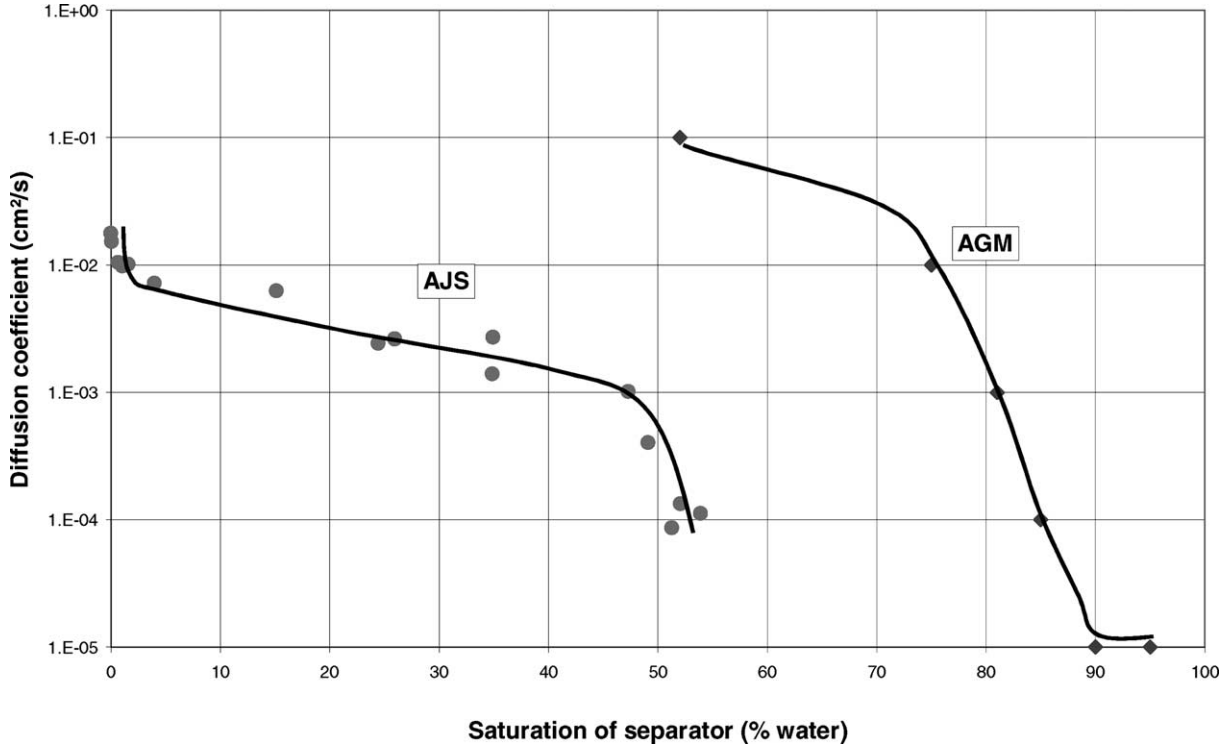

Fig. 8. Apparent diffusion coefficient of oxygen through AJS and AGM separators as a function of separator saturation.

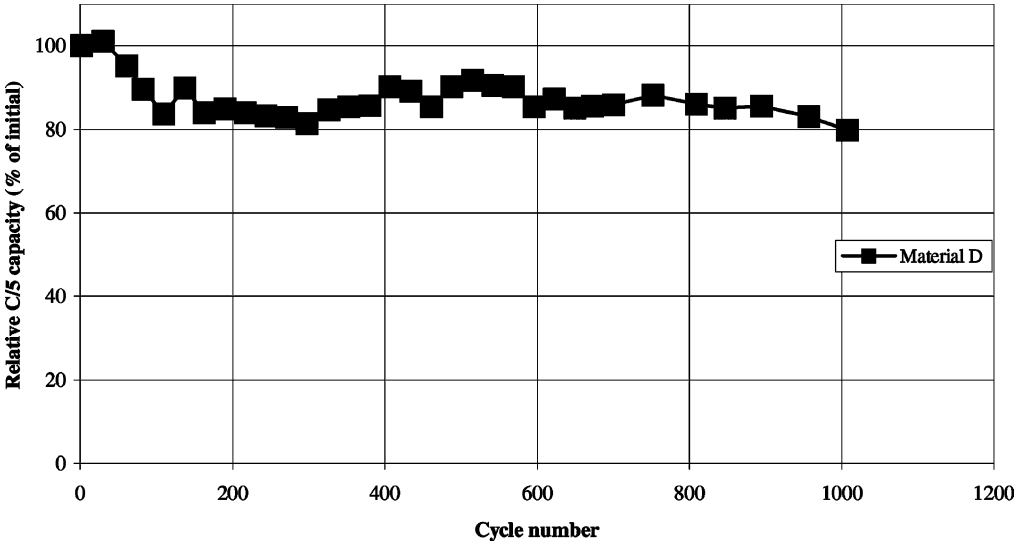

Fig. 9. Cycle life of a cell containing AJS as separator during 5 h rate cycling to 100% depth-of-discharge.

although some loss of capacity was attributable to a visible compaction of the negative active mass.

It is interesting to note that the discharge capacity of cells containing this separator were reported [11] to be sustained better at high rates than were those of cells containing gel.

3.3. Negative plate

Tests have continuously demonstrated [12] that cycle life of VRLA batteries in high power tests is significantly influenced by the performance of the negative plate. The negative active material (NAM) generally has a lower surface area than does the PAM and the key to obtaining good negative plate capacity over a long life has much to do with retaining as high a surface area of the NAM as possible. As has been pointed out already, it is important that the application of compressive forces to the plate stack in order to prevent expansion of the PAM should not simultaneously compact the NAM. An important role is also played by the organic expander materials which are routinely added to the negative paste mix. Without these the surface area of NAM falls quickly, leading to early plate failure. The adsorption of these organic materials on the electrochemically active surfaces in the plate exercises an important influence on the crystallization and reduction of lead sulfate and on the kinetics of hydrogen evolution.

It is clearly important that the expander materials should remain as effective as possible for the full working life of the battery. During periods of overcharge of VRLA cells, large quantities of oxygen arrive at the negative plate to be reduced and much heat is generated. Under these conditions, there is some concern about the durability of the traditional organic expanders (natural lignosulphonate products) [13] and research has been carried out both into the detailed function of these molecules and into the possibility of identifying more robust alternative materials. Cyclic voltammetry of cells containing a variety of different candidate expander materials [12] has provided two types of information.

(i) The efficiency of the expander, i.e. its ability to increase the capacity of a lead electrode, is indicated by the ratio of the of the area of the anodic peak in the presence of the expander compared to the area of the same peak in the absence of the expander.
(ii) The chargeability of the expander, i.e. the extent of the hindrance that the additive imposes on the charging process is indicated by the relative position of the cathodic peak with and without the expander present.

In general, those materials which offer a high level of efficiency are characterized by poor charge acceptance performance. The best overall performance in a negative plate is achieved with a compromise selection of materials with intermediate properties on both counts.

Different candidate expander materials exhibit quite different influences (overpotentials) on the rate of evolution of hydrogen at the potential to which the electrode is subjected during charge (Table 3) [14].

Table 3
Comparison of the gas evolution currents from negative plates with a variety of different organic expanders and at −1350 mV (versus Hg/$HgSO_4$ electrode), both before cycling and after 40 cycles

Expander	Gas evolution (mA) at −1350 mV, initial	Gas evolution (mA) at −1350 mV after 40 cycles
DD5	−6.3	−241.4
DD8	−9.7	−133.2
Kraftplex	−9.3	−392.6
N-17	−12.2	−46.3
S004	−11.4	−58
UP-414	−3.3	−144
Vanisperse A	−6.5	−81.6

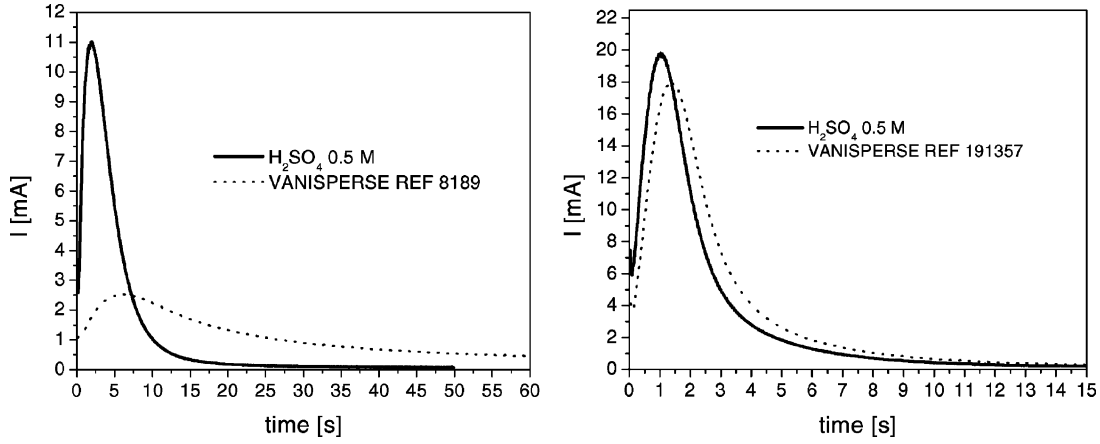

Fig. 10. Potentiostatic transients of cells with and without the addition of Vanisperse A. Material from batch V1 (on the left) affects the course of the chemistry following the transient far more than the material from batch V3 (on the right).

A noticeable feature of these measurements is the marked increase in the gassing current at −1350 mV after 40 cycles.

A set of three electrochemical techniques (electrochemical impedance, potentiostatic transients and cyclic voltammetry) was used to investigate the batch-to-batch variability of commonly used expander materials [14]. The three techniques all showed that for one of the materials (Vanisperse A), one batch out of three offered significantly lower effectiveness than the other two (e.g. Fig. 10). This variability of a product deriving from a natural origin may not be surprising and certainly lends impetus to the search for a synthetic alternative. During some tests, the synthetic Lomar B performed comparably with the natural products but in others, particularly at high rates, cells containing Lomar B did not perform so well. A further irony is that in most of the tests carried out Vanisperse out-performed the other materials tested.

There are some indications that some expanders function well early in plate life while others function better later. It is possible that a combination of expander materials may be able to provide a better overall performance than could any one material on its own.

In addition to the organic expander, negative active materials are generally provided with small amounts of barium sulfate and carbon black. Increases in the amount of carbon used, from 0.28 to 0.56% and then to 2.8%

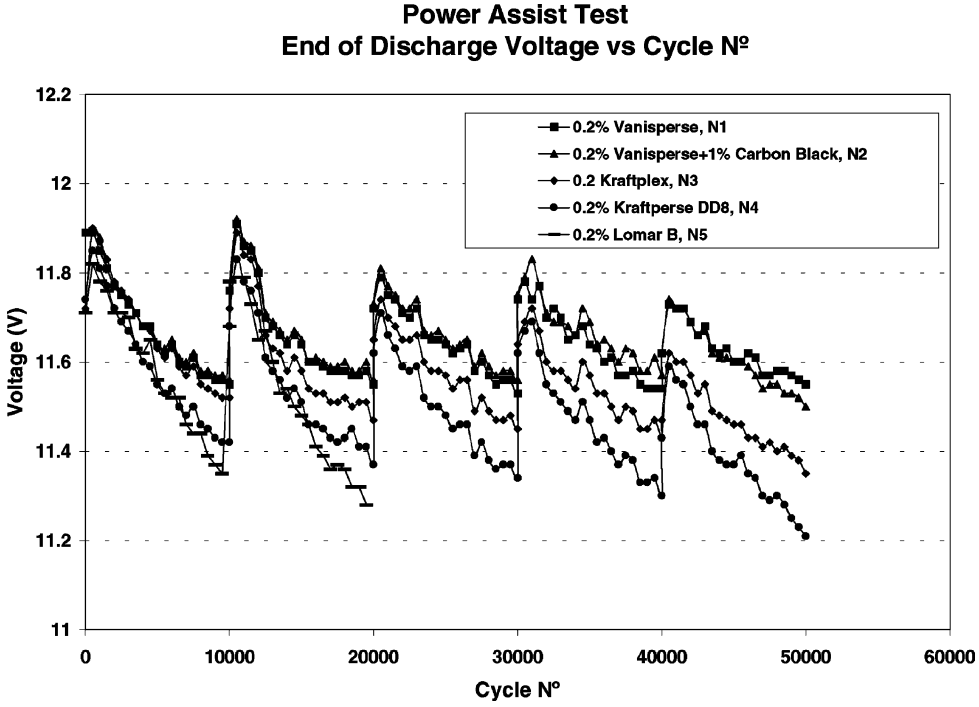

Fig. 11. EUCAR power-assist HEV cycling test on spiral wound battery designs with five different negative plate additive formulations.

produced marked increases in cycle life of a motorcycle battery under the ECE15L electric vehicle duty. Results from another ALABC project [15] have indicated that the form of carbon used is important as well as the amount. Carbon black may not be the optimum. When five different expander formulations, one with an increased level of carbon black combined with Vanisperse A, were separately incorporated into the negative plates of a spiral wound battery design, all behaved well in ECE15L cycling. The C5 capacity during this test remained above 80% of its initial value for at least 600 cycles for all five cases. When batteries with these same formulations were subjected to the power-assist HEV life cycle test according to the EUCAR specification four of the units completed 50,000 cycles [12] and it was clear that those with Vanisperse and Vanisperse plus extra carbon were capable of much more (Fig. 11).

It appears that continued attention to the type and quantities of the additives to the negative active material will be a profitable pursuit, but that it is unlikely to contribute as significant an improvement as the optimum choice of battery design.

4. Conclusions

The low corrosion rates of high-tin, antimony-free alloys can be exploited to reduce battery weight in pursuit of increase in specific energy. Care must be taken, however, to achieve and protect an adequate material bond at the grid/active material interface.

For deep discharge applications, once PCL-1 is avoided, the principal failure mechanism for up to around 1000 cycles (depending on rate) is softening of the positive active mass. The application of compression, together with the use of separator materials which help to sustain the compressive forces on the active materials, yields good results. Spiral wound designs are well suited to sustaining the compression of the positive active mass (PAM). Although high compressive forces must be applied to the PAM in order to obtain good deep cycle performance, it is important to avoid transmitting those forces to the negative active material, which loses capacity when compacted. Designs in which the negative plates are not over-pasted would appear to be most suitable from this point of view.

For float and partial-state-of-charge (PSoC) duty the requirements are different. PCL-2 is much less of a threat when the battery is not exposed to the large volume swings involved in deep discharge cycling. Management of the secondary reactions, particularly the oxygen cycle (reactions (5) and (7)) become all-important in order to avoid early failure through PCL-3 (in float or PSoC) or dry-out (in float). The negative plate stands up best if it is not exposed to too much overcharge, especially at high rate, when the kinetics of the competing reactions favor PCL-3.

Acknowledgements

The authors are grateful to the European Commission BRITE/EURAM program for financial support of the work described here and to all of the individual teams who carried out the experimental projects.

References

[1] D.A.J. Rand, R. Woods, R.M. Dell, Batteries for Electric Vehicles, Research Studies Press, 1998, ISBN 0-86380-205-0.
[2] D. Berndt, J. Power Sources 100 (2001) 29.
[3] A. Cooper, J. Power Sources 107 (2002) 245.
[4] K. McGregor, A.F. Holenkamp, M. Barber, T.D. Huynh, H. Ozgun, C.G. Phyland, A.J. Urban, D.G. Vella, L.H. Vu, J. Power Sources 73 (1998) 65.
[5] P.T. Moseley, J. Power Sources 95 (2001) 218.
[6] I. Dyson, EALABC project, Strategies for the further improvement of performance and life of lead–acid batteries for electric vehicles, BE97-4085, Task 2a.
[7] P.T. Moseley, R.D. Prengaman, J. Power Sources 107 (2002) 240.
[8] CMP, EALABC project, Strategies for the further improvement of performance and life of lead–acid batteries for electric vehicles, BE97-4085, Task 2b.
[9] University of Kassel, EALABC project, Strategies for the further improvement of performance and life of lead–acid batteries for electric vehicles, BE97-4085, Task 1a.
[10] Amer-Sil, Hollingsworth and Vose and Oldham France, EALABC project, Strategies for the further improvement of performance and life of lead–acid batteries for electric vehicles, BE97-4085, Task 1a.
[11] Daramic, Sonnenscein and ZSW, EALABC project, Strategies for the further improvement of performance and life of lead–acid batteries for electric vehicles, BE97-4085, Task 1b.
[12] Tudor and CLEPS, EALABC project, Strategies for the further improvement of performance and life of lead–acid batteries for electric vehicles, BE97-4085, Task 3.
[13] D. Pavlov, S. Gancheva, P. Andreev, J. Power Sources 46 (1993) 349.
[14] Politecnico di Torino, EALABC project, Strategies for the further improvement of performance and life of lead–acid batteries for electric vehicles, BE97-4085, Task 3.
[15] A.F. Hollenkamp, W.G.A. Baldsing, O.V. Lim, R.H. Newnham, D.A.J. Rand, J.M. Rosalie, D.G. Vella, L.H. Vu, ALABC, 2001, project N 1.2.